Supplementary Information For

Protonated Triplet-Excited Flavin Resolved by Step-Scan FTIR Spectroscopy: Implications for Photosensory LOV Domains

Christian Thöing, Anna Pfeifer, Sergej Kakorin, and Tilman Kottke*

Department of Chemistry, Physical and Biophysical Chemistry, Bielefeld University,
Universitätsstr. 25, D-33615 Bielefeld, Germany

* Corresponding author: tilman.kottke@uni-bielefeld.de.

Infrared Absorption Spectra of FMN Solutions

Absorption spectra of FMN were recorded to investigate a possible effect of pH or sucrose. All solutions were prepared in 50 mM sodium phosphate buffer. The corresponding buffer solution without FMN was used as reference. The overall band pattern of FMN in water did not change upon adding sucrose or lowering the pH from 8.0 to 3.2 (Fig. S1). All band positions are identical, with the exception of the C_2=O band. This band at 1661 cm^{-1} and pH 8.0 is generally very sensitive to the environment[1] and seems to be slightly shifted by ~3 cm^{-1} at pH 3.2.

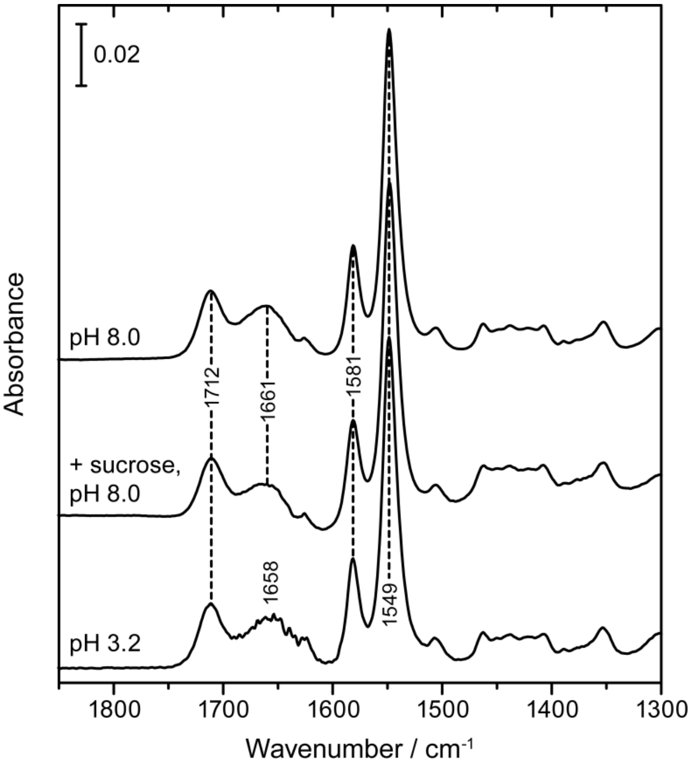

Figure S1: Infrared absorption spectra of FMN solutions. 44 mM FMN, pH 8.0 (top); 36 mM FMN, 40% (w/w) sucrose, pH 8.0 (middle); 14 mM FMN, pH 3.2 (bottom). The spectra were scaled to the same intensity of the band at 1549 cm^{-1}.

Difference Spectra of the Triplet-Excited States in the Region 1900-1800 cm^{-1} and Noise Level of the Experiments

Quantum chemical calculations on the neutral and protonated triplet-excited state of lumiflavin have predicted a significant upshift of a ring vibration upon protonation, which mainly involves CC and CN stretching vibrations.[2] In the calculated and scaled spectrum, this transition occurs at 1874 cm^{-1} with high intensity. However, the experimental spectra of the neutral and protonated triplet-excited state of FMN do not show any indication of an additional band in the spectral region between 1900 and 1800 cm^{-1} (Fig. S2).

In order to determine the noise level of the step-scan experiments, a difference spectrum was calculated from an intensity spectrum in the dark directly before laser excitation using the averaged preceding spectra in the dark as a reference (Fig. S2).

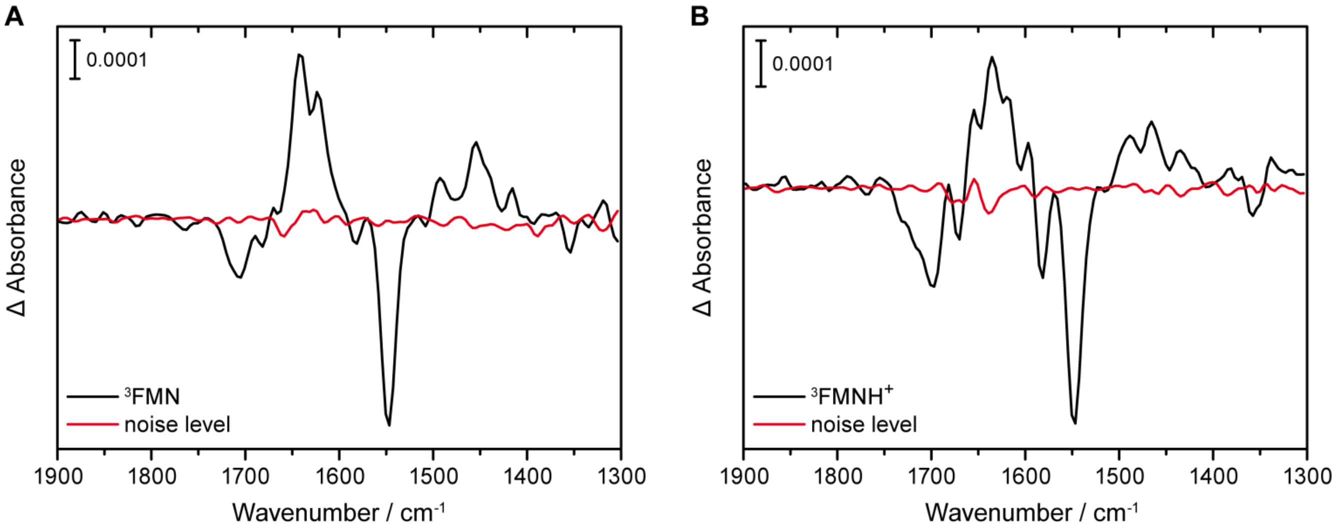

Figure S2: Infrared difference spectra of the (*A*) neutral and (*B*) protonated triplet-excited state of FMN (^{3}FMN and ^{3}FMNH$^+$, respectively) and the corresponding noise level. The difference spectra in the dark were scaled by the same factor as the spectra of the triplet-excited states.

Minor Additional Component in the Step-Scan Data Set of FMN at pH 8.0

Detailed analysis of the step-scan data revealed a second, minor component in some of the experiments (Fig. S3). The spectrum of this component is superimposed on the major band pattern of the triplet-excited state with an additional band at 1431 cm^{-1}. This band decays about twice as fast as the band at 1454 cm^{-1}. Furthermore, the negative band at 1581 cm^{-1} is completely compensated by an additional adjacent positive band at 1589 cm^{-1}. The C(4)=O band at 1643 cm^{-1} in the spectrum of the dominating component is upshifted to 1658 cm^{-1} by admixture of the minor component, which may point to reduced hydrogen bonding at the C(4)=O group. Taken together, these spectral differences might arise from the absorption of triplet-excited FMN dimers, which have been shown to be formed to some extent in aqueous solutions at millimolar concentrations.[3-5] Dimers are supposed to be formed by association of the isoalloxazine rings of FMN by hydrophobic interactions, which might influence the band pattern due to changes in polarity and hydrogen-bonding capacity. For further interpretation of these observations, the spectral characteristics of the FMN dimer need to be investigated systematically in the infrared.

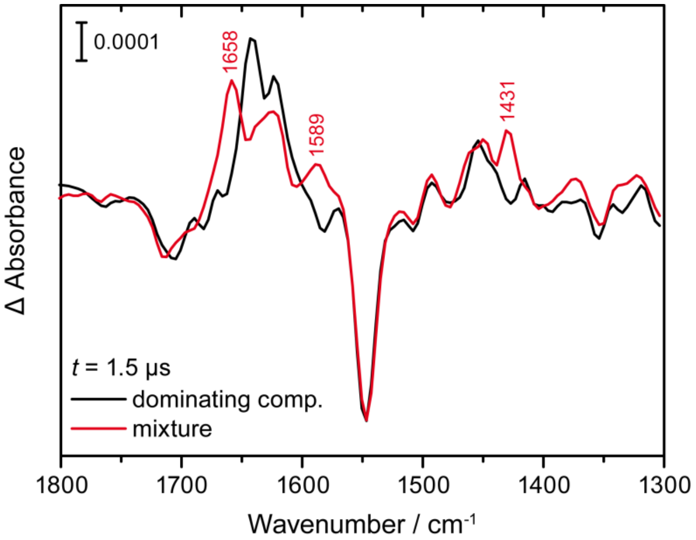

Figure S3: Dominating component and the admixture of a minor component in the step-scan data set of FMN measured in aqueous solution at pH 8.0. The dominating component is assigned to the triplet-excited state of free FMN molecules in solution, whereas the minor component might originate from the absorption of FMN dimers.

Decay Kinetics of the Anion Radical of FMN

The anion radical of FMN (FMN•$^{-}$) was produced by illuminating a solution of 20 mM FMN and 70 mM EDTA in 50 mM potassium phosphate buffer pH 9.0. In the step-scan data set, the kinetics of the band at 1550 cm^{-1} reveals that the oxidized state is partially recovered within 1 ms (Fig. S4). Fitting the 1550-cm^{-1} band kinetics with a second-order reaction yielded a rate constant of recovery of k_{1550} = 7.3×10^{7} M^{-1} s^{-1} (R^2 = 0.995). Disproportionation of FMN•$^{-}$ produces the fully reduced state (FMNH^{-}), as evidenced by the kinetics of the marker band at 1415 cm^{-1} (Fig. S4).

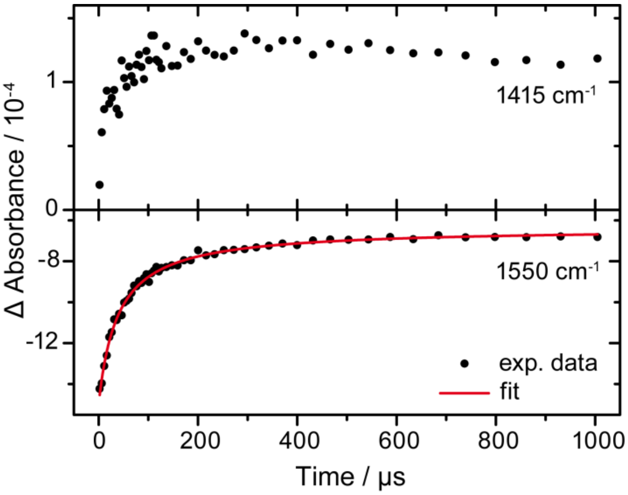

Figure S4: Time resolved step-scan data set of the photoreduction of FMN by EDTA. The kinetics of the band at 1415 cm^{-1} shows the formation of FMNH^{-} from FMN•$^{-}$ within 200 µs. At 1550 cm^{-1}, a partial recovery of the oxidized state of FMN was observed.

Quantum Chemical Calculations on Oxidized Lumiflavin and Its Triplet-Excited State

Lumiflavin (Lf) was chosen as a model compound for FMN. The geometry of lumiflavin was optimized in presence of different numbers of water molecules at varying starting positions. The final model (Fig. S5) was selected, because of the very good agreement in frequency and intensity of the calculated normal modes at 1729-1546 cm^{-1} with the experimental absorption spectrum of FMN in water[1] (Table S1). Modes below 1546 cm^{-1} cannot be directly compared due to the strong overlap with modes from the ribityl 5'-phosphate side chain of FMN. The optimized geometry of Lf with 4 H_2O was used as a starting structure for the optimization of geometry of lumiflavin in the triplet-excited state (^{3}Lf) (Fig. S6).

Density Functional Theory (DFT) and spin-unrestricted B3LYP were chosen for the geometry optimization and for calculation of frequencies of normal modes. B3LYP is the three-parameter gradient-corrected hybrid exchange functional proposed by Becke, Lee, Yang and Parr. DFT with B3LYP functional previously produced good results with low spin contamination in the normal mode analysis of ^{3}Lf in vacuum.[6,7] We applied the basis set 6-311+G(2d,p), which includes the diffuse functions important for molecules in excited states.

Potential energy distributions (PED) for the normal modes were calculated with a home-written algorithm in *Matlab* (The Mathworks, Natick, MA, USA) from the internal force constants and amplitudes of internal modes determined by *Gaussian03W*. Modes with more than 90% contribution from water molecules in the PED were not included in the further analysis of Lf. This cutoff was determined to eliminate water contributions in the spectrum of oxidized Lf, which were not observed in the experimental spectrum of FMN.[1]

The results of these calculations can be found on pages S7-S8 (Table S1 and S2).

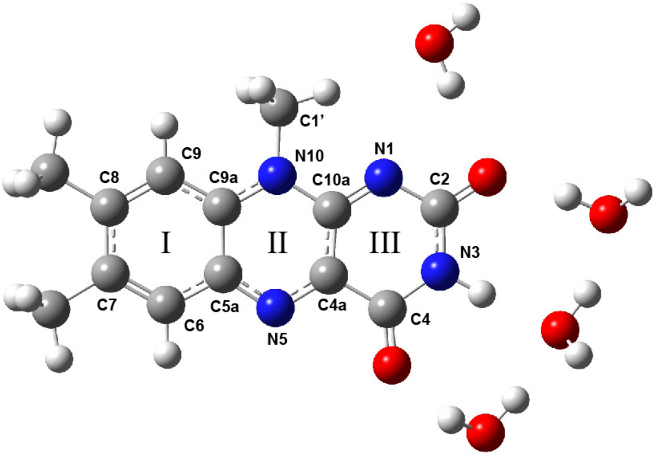

Figure S5: Optimized structure of oxidized Lf with four water molecules.

Table S1: Calculated frequencies (scaled by 0.98), intensities and potential energy distributions (PED) of the normal modes at 1800-1300 cm^{-1} of oxidized Lf. Comparison with the experimental difference spectrum of FMN (Fig. 2A, negative bands) and the absorption spectrum of FMN in water.[1] For simplification, only modes with an intensity >6% of the maximum intensity are shown. For the PED, a cutoff of 5% was applied.

Exp. Diff. / cm^{-1}	**Exp. Abs. / cm^{-1}**	**Theory / cm^{-1}**	**No.**	**Int.**	**PED component #1**	**PED component #2**	**PED component #3**
1709	1712	1729	103	347	90% νC4O[a]		
comp.[b]	1661	1677	102	559	82% νC2O	6% δN3H[a]	
comp.	1626	1629	99	80	62% νCC ring I	7% νCN ring II	6% δC6H
1581	1581	1576	96	772	35% νCN ring II	25% νCC ring I	9% νCN ring III
1547	1549	1546	95	1103	40% νCC ring I	20% νCN ring II	
comp.		1472	91	83	38% δC1’H_3	16% νCN ring II	12% δC8Me
comp.		1452	87	172	38% δN3H	26% νC2O	16% νC4O
1354		1385	81	143	19% δC8Me	19% δC1’H3	13% νCN ring III

[a] ν = stretching mode, δ = bending mode. [b] Band seems to be compensated in the experimental difference spectrum by strong contributions from ^{3}FMN (Fig. 2A).

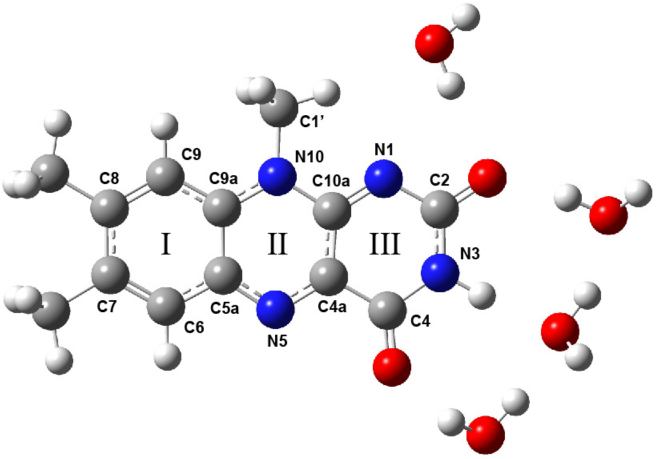

Figure S6: Optimized structure of the triplet-excited state of Lf with four water molecules.

Table S2: Calculated frequencies (scaled by 0.98), intensities and potential energy distributions (PED) of the normal modes at 1800-1300 cm^{-1} of ^{3}Lf. Comparison with the experimental difference spectrum of ^{3}FMN (Fig. 2A, positive bands). For simplification, only modes with an intensity >6% of the maximum intensity of Lf are shown (see Table S1). For the PED, a cutoff of 5% was applied.

Exp. / cm^{-1}	**Theory Lorentz / cm^{-1} [a]**	**Theory / cm^{-1}**	**No.**	**Int.**	**PED component #1**	**PED component #2**	**PED component #3**
1670	1665	1665	103	105	81% νC4O[b]	8% δN3H[b]	
1643	1634	1644	102	200	65% νC4O	26% νC2O	
		1635	101	208	55% νC4O	26% νC2O	12% δN3H
1624	1621	1624	100	239	83% νC2O	6% δN3H	
		1619	99	360	78% νC2O	10% δN3H	
comp.[c]	1601	1601	98	108	77% νC2O	8% δN3H	
comp.	1566	1566	97	385	59% νCC ring I	10% δC9H	
1493	1487	1488	95	294	24% νCN ring II	16% νCN1	14% νCC ring I
–[d]		1474	92	102	86% δC1'H_3		
1454	1463	1463	91	540	27% νCC ring I	25% δC8Me	11% νCN ring II
	1446	1446	89	123	35% νCC ring I	18% δC7Me	19% δC1'H_3
–[d]	1412	1412	85	284	67% δC1'H_3	6% νCC ring I	5% νCN ring II
1415	1378	1378	82	103	24% νCC ring I	21% νCN ring III	20% νCN ring II

[a] Band frequencies resulting from the convolution of the theoretical spectrum with Lorentzians (Fig. 2B). [b] ν = stretching mode, δ = bending mode. [c] Band seems to be compensated in the experimental difference spectrum by strong contributions from oxidized FMN. [d] Mode is not expected in the experimental difference spectrum of ^{3}FMN because it mainly originates from the N10 methyl group (C1'H_3) of Lf, which is substituted by ribityl 5'-phosphate in FMN.

References

1 M. Spexard, D. Immeln, C. Thöing and T. Kottke, *Vib. Spectrosc.*, 2011, **57**, 282-287.

2 M. T. Alexandre, T. Domratcheva, C. Bonetti, L. J. van Wilderen, R. van Grondelle, M. L. Groot, K. J. Hellingwerf and J. T. Kennis, *Biophys. J.*, 2009, **97**, 227-237.

3 Q. H. Gibson, V. Massey and N. M. Atherton, *Biochem. J.*, 1962, **85**, 369-383.

4 H. Grajek, R. Drabent, G. Zurkowska and C. Bojarski, *Biochim. Biophys. Acta*, 1984, **801**, 456-460.

5 H. Grajek, G. Zurkowska, R. Drabent and C. Bojarski, *Biochim. Biophys. Acta*, 1986, **881**, 241-247.

6 C. B. Martin, X. F. Shi, M. L. Tsao, D. Karweik, J. Brooke, C. M. Hadad and M. S. Platz, *J. Phys. Chem. B*, 2002, **106**, 10263-10271.

7 C. B. Martin, M. L. Tsao, C. M. Hadad and M. S. Platz, *J. Am. Chem. Soc.*, 2002, **124**, 7226-7234.